Available online at www.sciencedirect.com
SCIENCE DIRECT®
Journal of Electrostatics 64 (2006) 498–505
Journal of ELECTROSTATICS
www.elsevier.com/locate/elstat

EHD flow in a wide electrode spacing spike–plate electrostatic precipitator under positive polarity

J. Podliński[a], J. Dekowski[a], J. Mizeraczyk[a,*], D. Brocilo[b], K. Urashima[b], J.S. Chang[b]

[a]*Centre for Plasma and Laser Engineering, The Szewalski Institute of Fluid Flow Machinery, Polish Academy of Sciences, Fiszera 14, 80-231, Gdańsk, Poland*
[b]*Department of Engineering Physics, McMaster University, Hamilton, Ont., Canada L8S 4L7*

Available online 4 November 2005

Abstract

In this work, results of two- and three-dimensional particle image velocimetry (PIV) measurements of the flow velocity fields in a wide spacing spike–plate electrostatic precipitator (ESP) under positive polarity are presented. A DC voltage of positive polarity (up to 28 kV) was applied to the spike electrode. The average gas flow velocity was 0.6 m/s. The PIV measurements were carried out in four planes perpendicular to the plate electrodes. Three parallel planes passed along the ESP while one plane passed across the ESP duct. The results show that electrohydrodynamic (EHD) secondary flow with relatively strong vortices exist in the ESP. The EHD secondary flow pattern depends on applied voltage and measuring plane position in respect to the spike tip. The strongest vortices occur in the plane passing through the tip of the upstream-directed spike. These relatively strong EHD vortices may hinder collection of the particles in the diameter range of 0.1–1 μm in the wide electrode spacing spike–plate ESPs.

Keywords: Electrostatic precipitator; EHD flow; PIV measurements

1. Introduction

Electrostatic precipitators (ESPs) are being widely used as dust particle collectors due to their high total particle collection efficiency (99.9%) with a low-pressure drop. However, the collection efficiency of particles of submicron size is relatively low [1].

An ESP modeling and measurements performed downstream of full-scale ESPs show that the dust particle collection efficiency depends on the gas flow velocity, applied voltage, particle physical parameters, electrode geometry and on the EHD secondary flow [2–4]. The most difficult to collect are particles in diameter range of 0.1–1 μm, with a maximum for particles having a diameter of about 0.5 μm.

The influence of the EHD secondary flow on the collection efficiency has been debated for decades. The results of the modelling of particle collection efficiency [2] suggest that the particle collection could be significantly improved if the EHD secondary flow were eliminated. Consequently, improvements in the geometry and operating conditions in ESPs should be performed to reduce the EHD secondary flow in them.

One of the proposals for eliminating the EHD secondary flow in ESPs is the use of a spike discharge electrode. However, there is a lack of information on the EHD secondary flow in the ESPs with such an electrode arrangement.

Recently, the particle image velocimetry (PIV) technique has become a powerful tool for measuring the flow patterns in ESPs. In [5,6] the PIV measurements were focused on the existence of EHD secondary flow in wide electrode spacing ESPs under positive polarity, which, according to the modelling presented by Kogelschatz et al. [2], influences the collection efficiency of submicron particles. The relatively wider spacing ESP operation was chosen since such an ESP can be applied to the collection of high resistivity dust particles [1]. The ESP operation under positive polarity was used because of the relatively low ozone generations and the potential for the reduction of NO_x and SO_x.

*Corresponding author.
E-mail address: jmiz@imp.gda.pl (J. Mizeraczyk).

0304-3886/$ - see front matter © 2005 Elsevier B.V. All rights reserved.
doi:10.1016/j.elstat.2005.10.004

In this work, results of two- and three-dimensional PIV measurements of the flow velocity fields in a positively polarized wide spacing spike–plate ESP are presented. The measurements were focused on existence of the EHD secondary flow.

The PIV measurements were carried out in four planes placed perpendicularly to the plate electrodes. Three different parallel planes passed along the ESP by the upstream- and downstream-directed spike tips, as well as in-between them. This allowed us to study the influence of the spike on the velocity field in the ESP. The fourth measuring plane passed across the ESP duct. In this case three-dimensional PIV measurements were carried out.

2. Experiment

The apparatus used in this experiment consisted of an ESP, high voltage supply and standard PIV equipment for the measurement of velocity fields (as presented by Mizeraczyk et al. [5,6]).

The ESP was a plane-parallel acrylic duct, 1000 mm long, 200 mm wide and 100 mm high. At the top and bottom of the duct two collecting stainless-steel plate electrodes (200 mm × 600 mm) were placed. In the middle of the ESP the spike electrode (200 mm long, 1 mm thick, and 30 mm tip-to-tip wide) was mounted in the acrylic sidewalls, parallel to the plate electrodes (Fig. 1). The spike tips were directed upstream on the one side of the electrode, and downstream on the other. The distance from the spike electrode to the plate electrodes was 50 mm.

The positive voltage applied to the spike electrode was up to 28 kV, the discharge current was up to 210 μA. The voltage was supplied to the spike electrode through a 10 MΩ resistor.

Air flow seeded with fine TiO_2 particles (size of less than 1 μm) was blown along the ESP duct with an average velocity of 0.6 m/s.

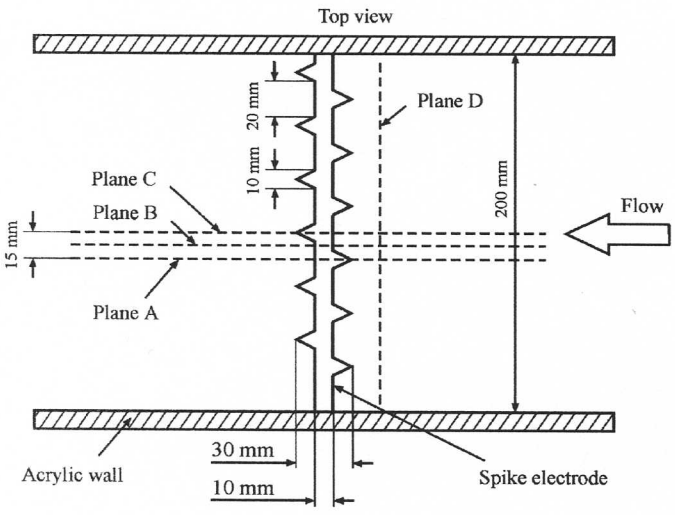

Fig. 1. Top-view schematic drawing of the spike–plate ESP.

The PIV measurements were carried out in four planes—A, B, C and D, all placed perpendicularly to the plate electrodes (Fig. 1). Three planes were fixed along the ESP duct. The first of them (plane A) passed through the tip of the upstream-directed central spike electrode, the second plane (plane B) passed in-between the upstream and downstream spikes, while the third plane (plane C) passed through the tip of the neighbouring downstream-directed spike electrode. The fourth plane (plane D) was placed across the ESP duct, 15 mm before the upstream-directed spike tips.

The flow velocity field maps [area of 260 mm × 100 mm] obtained in planes A, B and C were composed of three adjacent overlapping velocity fields [area of each 100 mm × 100 mm]. All the velocity fields resulted from the averaging of 100 measurements, which means that each velocity map was time-averaged. Based on the measured velocity fields, the apparent flow streamlines of a hypothetical two-dimensional flow were calculated and presented in this paper.

3. Results

Figs. 2–5 show the flow streamlines in the spike–plate ESP at a primary flow average velocity of 0.6 m/s. At this velocity the Reynolds number was $Re = V \times L/v = 4000$ (the parameters used to calculate Re were: the primary flow velocity $V = 0.6\,\mathrm{m/s}$, characteristic length (plate–plate distance) $L = 0.1\,\mathrm{m}$, and air dynamic viscosity $v = 15 \times 10^{-6}\,\mathrm{m^2/s}$).

The flow streamlines in the plane A (without voltage) are shown in Fig. 2. As can be seen, the flow is uniform in the whole measured area with a slight disturbance near the spike electrode. Very similar results were obtained in planes B and C.

When the applied voltage exceeded corona onset (about 11 kV) the flow pattern changed significantly, depending on applied voltage. Figs. 3–5 show the flow streamlines in the planes A, B and C, respectively, for three selected voltages: 15.6, 23.8 and 27.9 kV. The total discharge current was 40, 120 and 210 μA, respectively. Thus the electrohydrodynamic numbers [Ehd $= I \times L^3/(v^2 \times \rho \times \mu_i \times A)$] [7], based on the flow channel data, were 1.26×10^7, 3.78×10^7 and 6.61×10^7, respectively. Hence, the ratios of the Ehd number to the Reynolds number squared (Ehd/Re^2) were: 0.8 (for 15.6 kV—Figs. 3a, 4a and 5a), 2.4 (for 23.8 kV—Figs. 3b, 4b and 5b) and 4.2 (for 27.9 kV—Figs. 3c, 4c and 5c). The parameters used to calculate Ehd were: the total discharge current I, characteristic length (plate–plate distance) $L = 0.1\,\mathrm{m}$, air dynamic viscosity $v = 15 \times 10^{-6}\,\mathrm{m^2/s}$, air density $\rho = 1.205\,\mathrm{kg/m^3}$, ion mobility ($N_2^+$ in air) $\mu_i = 2.93 \times 10^{-4}\,\mathrm{m^2/Vs}$, and discharge area (100 mm long and 200 mm wide discharge area on the two plate electrodes) $A = 2 \times 100\,\mathrm{mm} \times 200\,\mathrm{mm} = 0.04\,\mathrm{m^2}$. The uniform current distribution on the plate electrodes was assumed. This assumption was justified by the optical emission intensity measurements of the discharge from the

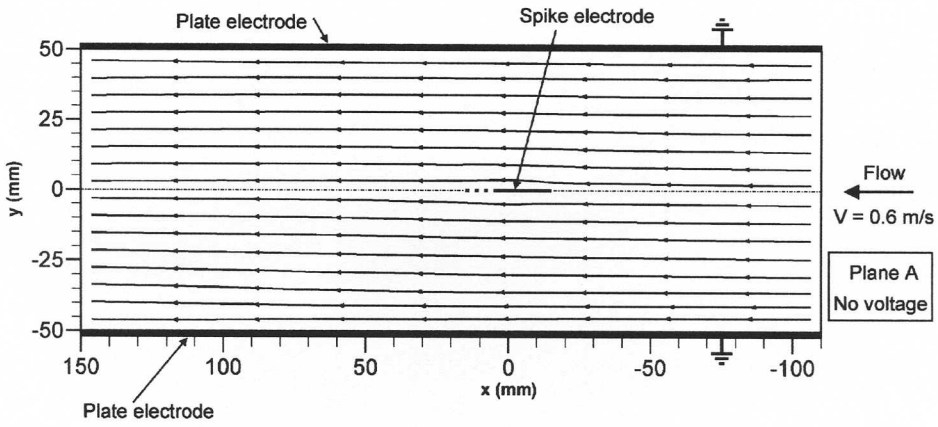

Fig. 2. Flow streamlines in the plane A for the spike–plate ESP at the averaged main flow velocity of 0.6 m/s. No voltage applied. The Reynolds number $Re = 4000$.

spike electrode (observation of N_2 second positive band emission which is proportional to the electron density) [8].

Generally, when the applied voltage is increased, the EHD force (equal to ρE per volume unit, where ρ is the ion density, E is the electric field) moves the ions, causing strong secondary flow which alter significantly the original, primary flow. Usually the EHD secondary flow increases with increasing applied voltage (or discharge current), and hence EHD number. Since the current flux and the electric field are three dimensional, three-dimensional vortex structures are generated in the flow. The influence of the travelling ions on the flow structures for needle–plate cases (needle perpendicular to the plate) was widely discussed by Sigmond et al. [9] and Zhao et al. [10]. However, the present spike electrode is parallel to the grounded planes. Therefore, three-dimensional structures of the electric field as well as current flux distribution have to be expected in the investigated ESP.

The evolution of the vortex structures in the plane A (passing through the tip of the upstream-directed central spike electrode) with increasing applied voltage is shown in Fig. 3. At 15.6 kV (Fig. 3a), vortex structures near the upstream tip started to develop. The upper and lower vortex structures are not identical likely due to small asymmetries in the positioning of the spike electrode with respect to the plate electrodes and due to a certain asymmetry of the primary flow profile at the ESP inlet (found in the vector velocity field, not shown). The asymmetry of the vortex structures is higher at lower applied voltages. As can be seen in Fig. 3, even the weak upstream vortices formed in the upstream region (in respect to the spike electrode) start to block the primary gas flow in the central part of the ESP and cause the flow to move nearer both plate electrodes. In the downstream region the influence of the EHD forces on the flow is less pronounced. With increasing voltage new vortices appear in the downstream region, while the upstream vortices became stronger. At 23.8 kV (Fig. 3b) the downstream pair of vortices is clearly developed and the upstream vortex pair occupies almost the whole ESP height. The fully developed pairs of strong vortices covering the whole ESP height in the upstream region (with their centres at $x = -15$ mm) and in the downstream region ($x = 30-40$ mm) appear at 27.9 kV (Fig. 3c). The upstream vortices block the main flow and force it to move very close to the plate electrodes. On the other hand, the downstream vortices do not allow the main flow to move near the plate electrodes. As a result, after passing the spike electrode the main flow turns towards the ESP centre and passes between the downstream vortices.

Two pairs of vortices, upstream and downstream, develop also in the plane B (Fig. 4), which is fixed in the midway between the upstream- and downstream-directed spikes (Fig. 1). However, the vortices in this plane are smaller than those in the plane A, even at 27.9 kV. The direction of the main gas flow is similar as in the plane A.

The influence of the EHD forces on the flow patterns in the plane C, passing through the tip of the downstream-directed spike electrode (Fig. 1), is lower than that in the planes A and B (Fig. 5). Only a slight disturbance of the uniform primary flow is seen at 15.6 kV (Fig. 5a). For higher voltages, relatively small vortex structures close to the spike electrode and in the downstream ESP region are present (Figs. 5b and c). Therefore, even at 27.9 kV a considerable part of the primary flow moves not much disturbed by the EHD forces to the ESP outlet.

The stronger vortices, visible in Figs. 3–5 appear for higher applied voltages, i.e. for higher Ehd numbers. However, the strength and dimension of the vortices depend also on the directions of the EHD secondary flow and the primary flow with respect to each other. If they are opposite, stronger vortices develop.

Comparing the EHD secondary flow in planes A, B and C for relatively high voltages (23.8 and 27.9 kV), we can find that the pairs of vortices in the plane A are strongest, although the Ehd numbers in the planes A and C are the same. This difference is a result of a strong interaction of the upstream-directed EHD secondary flow from the

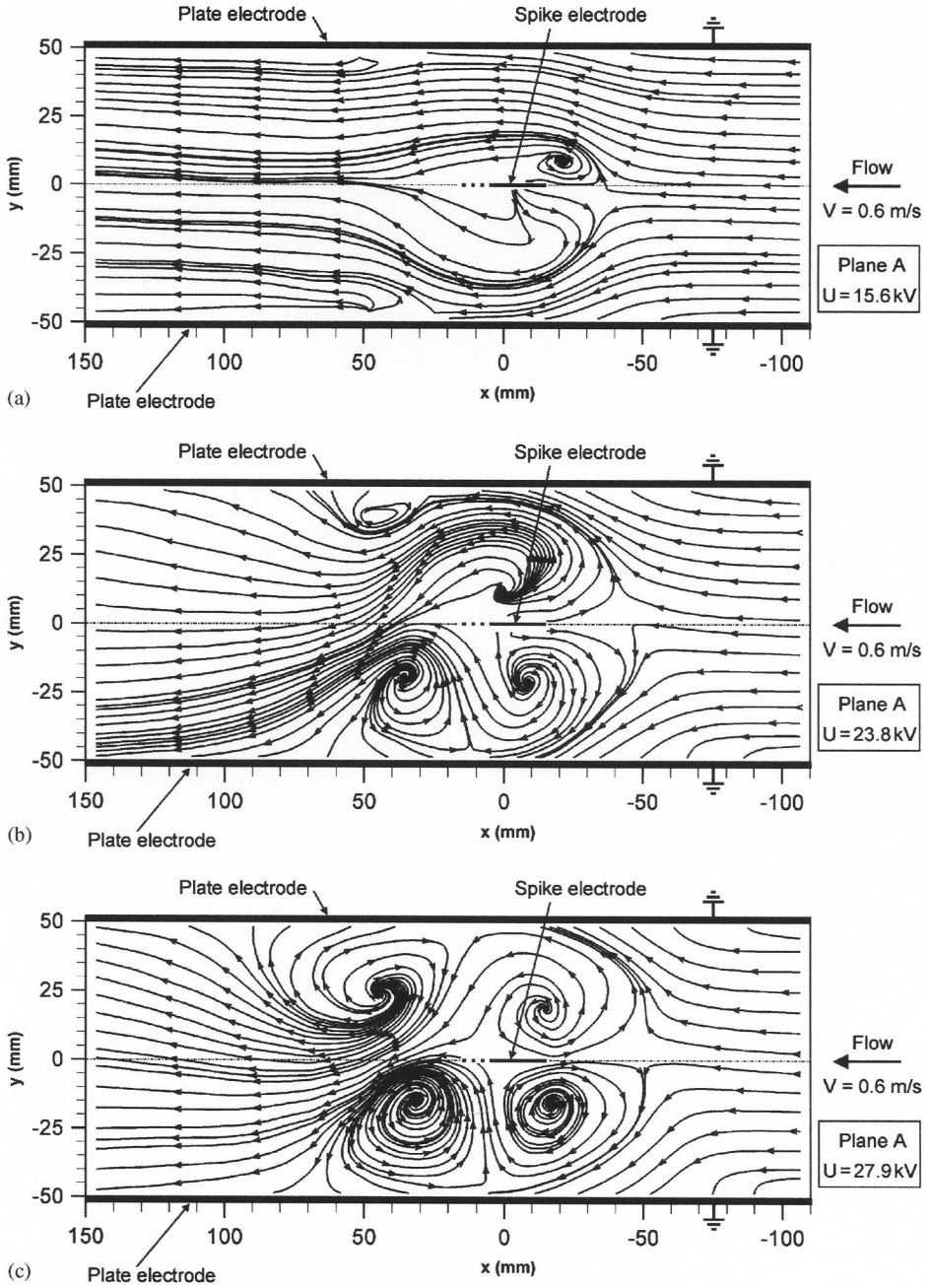

Fig. 3. Flow streamlines in the plane A for the spike–plate ESP at the averaged main flow velocity of 0.6 m/s. Applied DC positive voltage: (a) 15.6 kV, (b) 23.8 kV and (c) 27.9 kV; averaged discharge current: 40, 120, 210, respectively. The Reynolds number $Re = 4000$ and Ehd numbers are 1.26, 3.78 and 6.61×10^7, respectively.

upstream spike tip in the plane A with the oppositely directed primary flow. This strong interaction causes the strong vortices observed in the plane A. On the other hand, in the plane C the directions of the EHD secondary flow and the primary flow are in accord. Therefore, their interaction is weaker and the downstream flow pattern is less disturbed.

The measurements in the planes A, B and C showed that the flow pattern depends on whether the measuring plane contains a discharge source (i.e. the spike tip) or not. Therefore, using a local Ehd number for each plane would be more adequate to describe the EHD secondary flow than the use of the average Ehd number as used in this work.

Analyzing the two-dimensional flow patterns presented in Figs. 3–5 one may deduce that the flow in the presented spike–plate ESP is strongly three-dimensional, as it has been predicted by numerical modelling [2,11]. This was confirmed by results of three-dimensional measurements (Fig. 6), carried out in the plane D (i.e. perpendicular to the

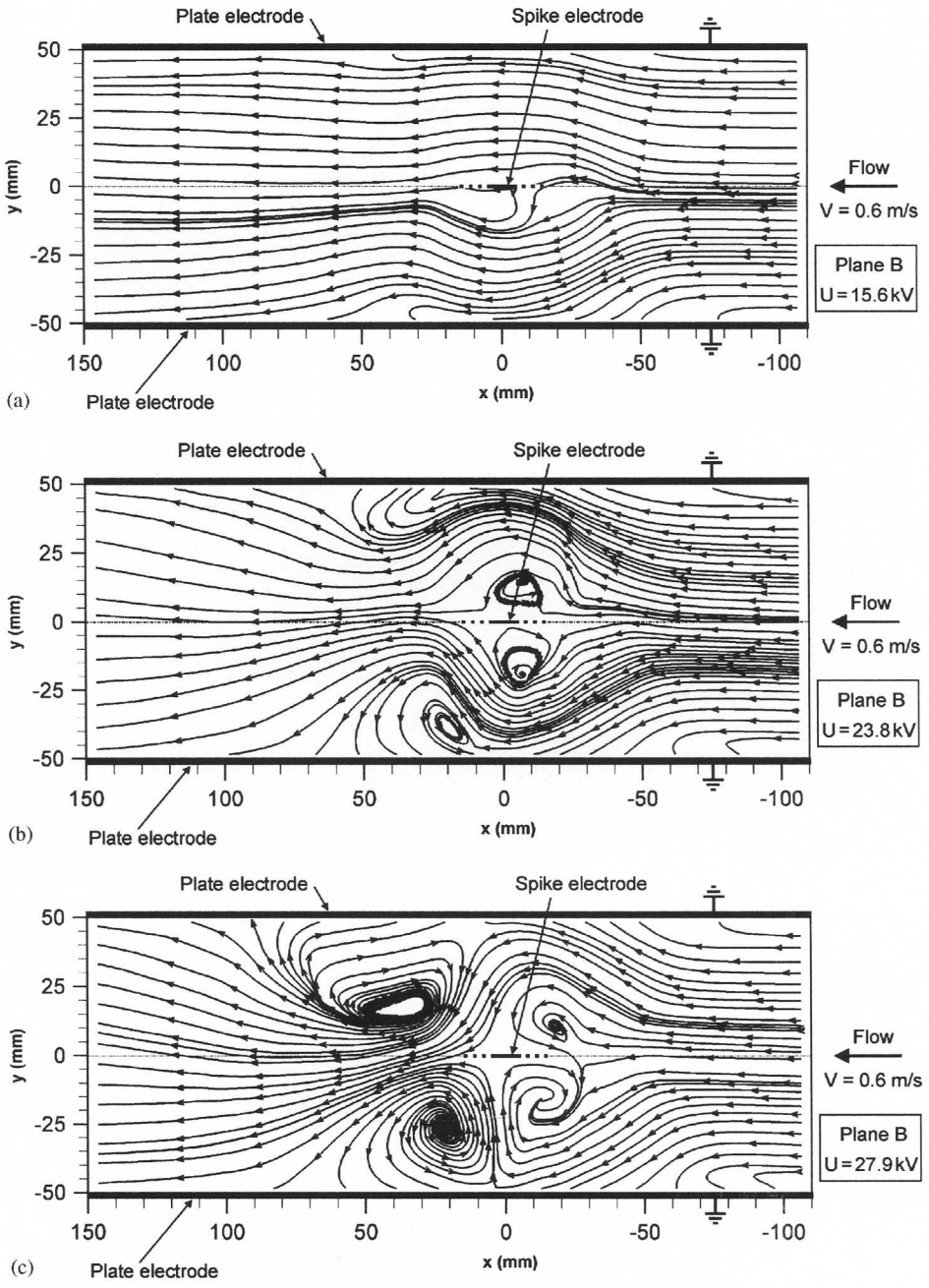

Fig. 4. Flow streamlines in the plane B for the spike–plate ESP for the conditions as in Fig. 3.

primary flow direction). As can be seen in Fig. 6a, the flow velocities which are perpendicular (y, z directions) to the primary flow direction are considerable. The y-component of the velocity reaches values up to 0.8 m/s while the velocity z-component is up to 0.3 m/s in the vicinity of the central spike tips and even higher than 1 m/s in the vicinity of the acrylic side walls. The sidewalls considerably disturb the flow around the nearest spike tips. However, the flow patterns around the central spike tips are stable and very similar to each other (Fig. 6b). The flow velocity component in the x direction (the primary flow direction) in the plane D is shown in Fig. 6c. The x-component velocities reach values from 0.7 m/s in the opposite direction to the primary flow direction (in the planes passing through the upstream-directed spike tips—like plane A) to 1.4 m/s in the primary flow direction (in the planes passing through the downstream-directed spike tips—like plane C).

It can be deduced from Figs. 3–6 that a transversely directed-to-the primary flow three-dimensional conical tornado-like vortices are developed in the ESP. At the upstream region of the ESP the conical tornado-like vortices have their vertices in the plane C, and their bases in the plane A.

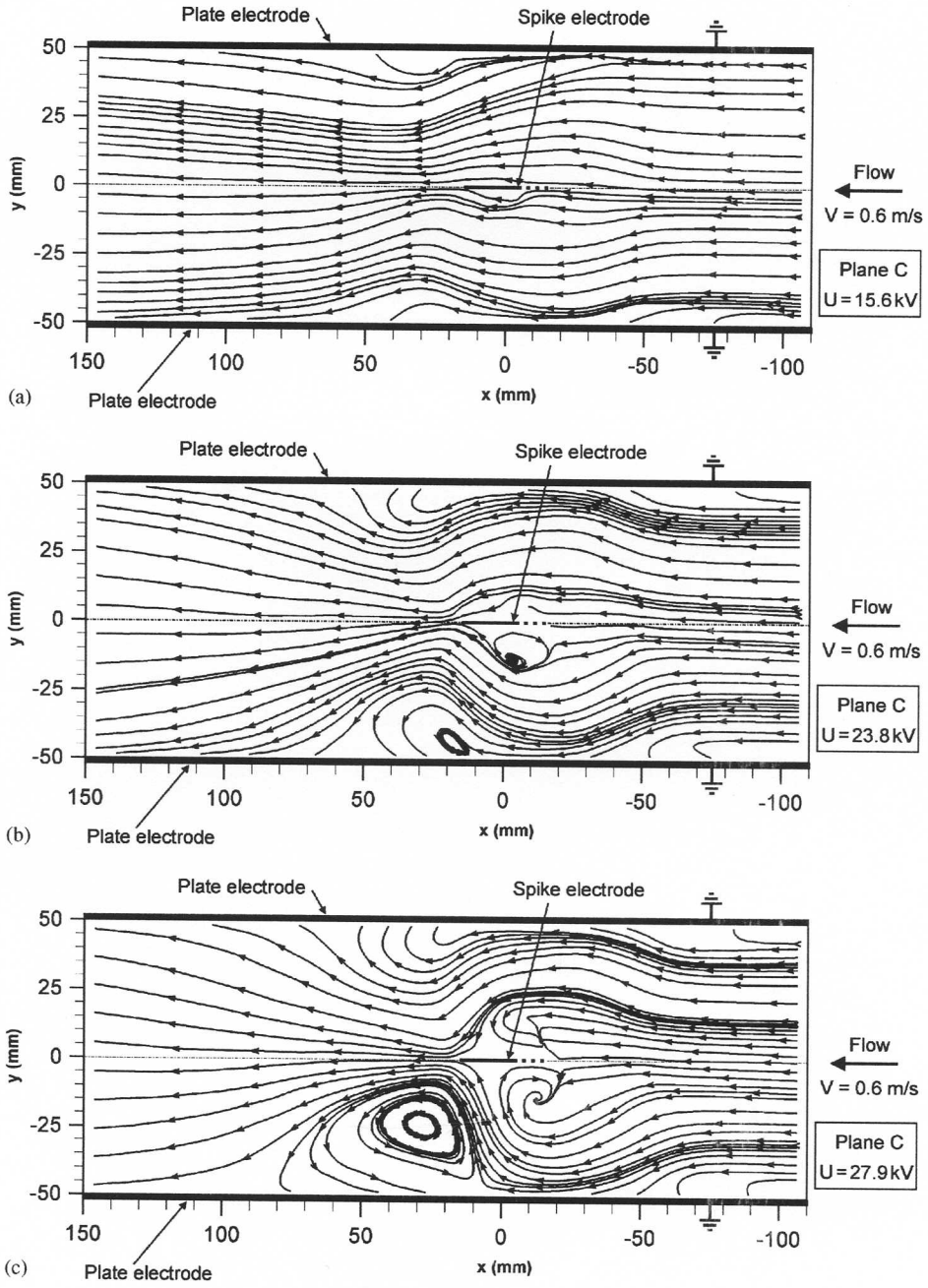

Fig. 5. Flow streamlines in the plane C for the spike–plate ESP for the conditions as in Fig. 3.

4. Summary and conclusions

In this paper, results of the two- and three-dimensional PIV measurements of the flow velocity fields in a positively polarized spike–plate ESP are presented. The measurements were carried out in four different planes, fixed perpendicularly to the plate electrodes, along and perpendicular to the direction of the primary flow.

The results show that:

- the EHD secondary flow do exist in the spike–plate ESP,
- the EHD secondary flow interacts strongly with the primary flow, forming relatively strong EHD vortices, in particular in the upstream region of the spike electrode,
- the strongest vortices appear in the plane passing through the upstream-directed spike (plane A),
- the diameter of the vortices increases with increasing voltage, i.e. with increasing Ehd number,
- the flow patterns in the planes A, B and C are different. This results from differently directed spikes in the planes A and C, in respect to the primary gas flow, and from the lack of the corona discharge source (no spike on the electrode) in the plane B,
- from the flow patterns in the planes A, B and C one may deduce that there exist the conical tornado-like vortices,

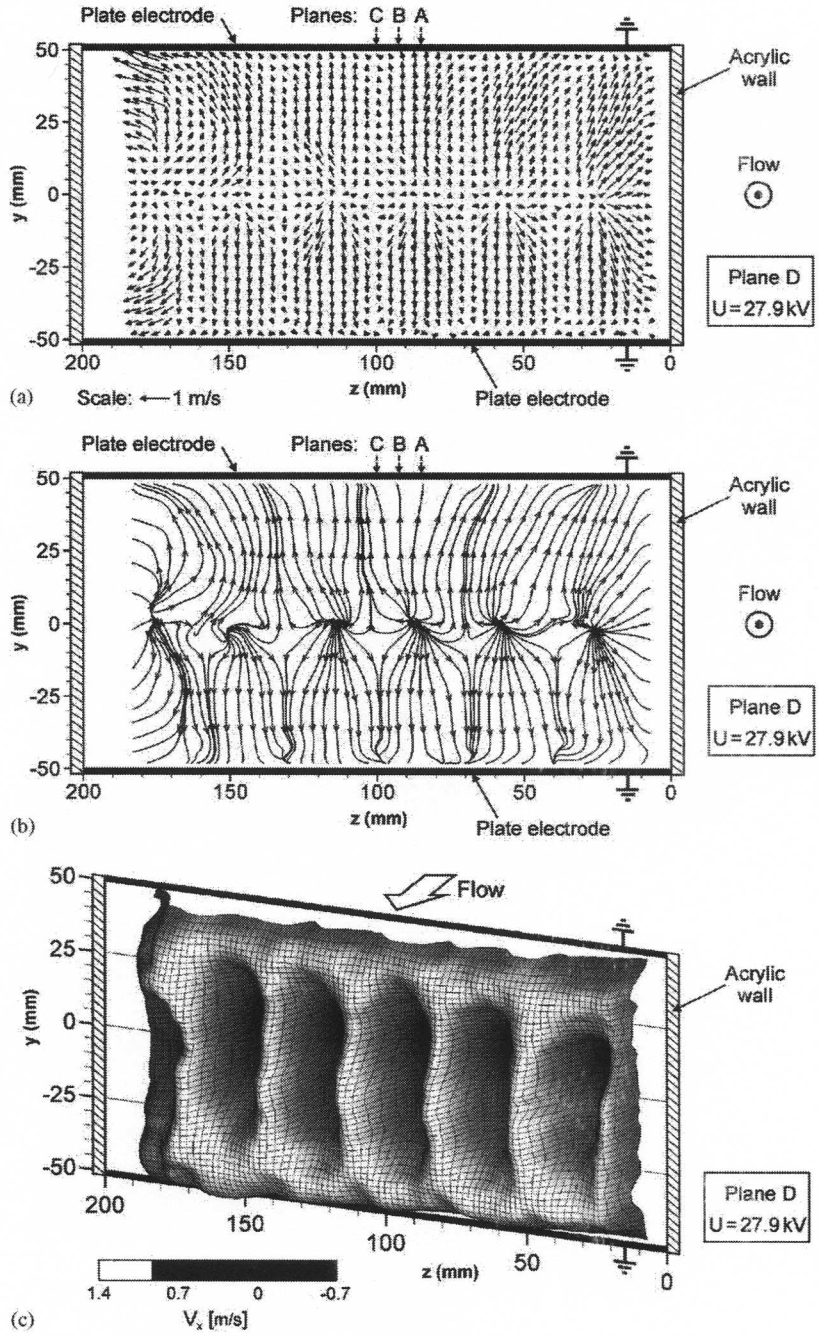

Fig. 6. Three-dimensional measurement in the plane D for the spike–plate ESP for the conditions as in Fig. 3c. Flow velocity field in the y–z plane (plane D) (a), corresponding flow streamlines (b) and x-component of the flow velocity (c).

located perpendicularly to the primary flow. This means that the flow in the spike–plate ESP is three dimensional, which was confirmed by the three-dimensional PIV measurements.

Acknowledgements

This work was supported by the Foundation for Polish Science (FNP, subsidy 8/2001), the State Committee for Scientific Research (Grant KBN PB 1756/T10/01/21) and the Natural Sciences and Engineering Counsel of Canada. The authors would like to thank Dr. R.D. Findlay, Prof. T. Ohkubo, Prof. S. Kanazawa, and Prof. T. Yamamoto for their stimulating discussions and suggestions.

References

[1] A. Mizuno, IEEE Trans. Diel. Electr. Insul. 7–5 (2000) 615–624.
[2] U. Kogelschatz, W. Egli, E.A. Gerteisen, ABB Rev. 4 (1999) 33–42.
[3] D. Brocilo, J.S. Chang, R. Godard, A. Berezin, J. Aerosol Sci. 30–1 (1999) 855–856.

[4] P. Atten, F.M.J. McCluskey, A.C. Lahjomri, IEEE Trans. Ind. Appl. 23–4 (1987) 705–711.
[5] J. Mizeraczyk, M. Kocik, J. Dekowski, M. Dors, J. Podliński, T. Ohkubo, S. Kanazawa T. Kawasaki, J. Electrostat. 51–52 (2001) 272–277.
[6] J. Mizeraczyk, J. Dekowski, J. Podliński, M. Kocik, T. Ohkubo, S. Kanazawa, J. Visualization 6 (2) (2003) 125–133.
[7] IEEE-DEIS-EHD Technical Committee, IEEE Trans. Diel. Electr. Insul. 10–1 (2003) 3–6.
[8] D. Brocilo, J.S. Chang, R.D. Findlay, IEEE Conference Record Abstracts, 30th International Conference on Plasma Science, 2003, p. 254.
[9] R.S. Sigmond, A. Goldman, M. Goldman, Proceedings of the 10th International Conference on Gas Discharges and Their Applications, Swansea, UK, 1992, pp. 330–333.
[10] L. Zhao, K. Adamiak, J. Electrostatics 63 (3–4) (2004) 337–350.
[11] T. Yamamoto, M. Okuda, M. Okubo, IEEE Trans. Ind. Appl. 39 (2003) 1602–1607.